Differential impact cratering of Saturn's satellites by heliocentric impactors

Hirata, Naoyuki

(Citation)
Journal of Geophysical Research: Planets,121(2):111-117

(Issue Date)
2016-02

(Resource Type)
journal article

(Version)
Version of Record

(URL)
https://hdl.handle.net/20.500.14094/90003438

AGU PUBLICATIONS

JGR

Journal of Geophysical Research: Planets

RESEARCH ARTICLE
10.1002/2015JE004940

Key Points:
- The distribution of impact craters on Rhea and Iapetus
- The larger craters show an apex-antapex asymmetry, while the smaller craters show no asymmetry
- This difference is likely caused by two distinct impactor populations

Supporting Information:
- Tables S1–S11 and Figures S1–S3
- Table S1
- Table S2

Correspondence to:
N. Hirata,
hirata@tiger.kobe-u.ac.jp

Citation:
Hirata, N. (2016), Differential impact cratering of Saturn's satellites by heliocentric impactors, *J. Geophys. Res. Planets*, *121*, 111–117, doi:10.1002/2015JE004940.

Received 14 SEP 2015
Accepted 12 JAN 2016
Accepted article online 14 JAN 2016
Published online 15 FEB 2016

Differential impact cratering of Saturn's satellites by heliocentric impactors

Naoyuki Hirata[1]

[1]Graduate School of Science, Kobe University, Kobe, Japan

Abstract Saturnian satellites are thought to have been struck by two different types of impactors: those with heliocentric origins and those with planetocentric origins. Many of the impacts are suggested to come from planetocentric debris, while many crater count studies assume an ecliptic comet origin when determining the ages of the surfaces. To assess the contribution of planetocentric impactors, this study examines the global distribution and apex-antapex asymmetry of impact craters on Rhea and Iapetus. The results demonstrate that the craters of Rhea (more than 20 km in diameter) and Iapetus (more than 30 km in diameter) show an apex-antapex asymmetry. This suggests that most of the large craters are formed from heliocentric impacts. In contrast, the craters less than 20 km in diameter seem to show no asymmetry. Possible explanations for this are either planetocentric impactor origins or saturation with impact craters.

1. Introduction

The origin of the Saturnian satellite impactors is uncertain. Determining the sources of the impactors is critical for the estimation of the surface age of an object and the assessment of the dynamic evolution of the outer solar system. *Dones et al.* [2009] concluded that the potential impactors in the Saturn system could be divided into (a) main belt asteroids, (b) Trojans of Jupiter or Neptune, (c) ecliptic comets, (d) nearly isotropic comets, (e) secondary or sesquinary impactors ejected from a primary impact, and (f) Saturn's own irregular satellites. In general, heliocentric (Sun-orbiting) objects such as items (b)–(d) play a major role as primary impactors and generate numerous secondary or sesquinary impact objects [e.g., *Bierhaus et al.*, 2012]. However, the majority of the craters in the Saturn system may have been formed by planetocentric (planet-orbiting) impactors, such as items (e) and (f), based on the abundance of small craters and the global uniformity of cratering [*Dones et al.*, 2009].

In order to assess the effect of planetocentric cratering, this study investigates the apex-antapex asymmetry of cratering in the Saturn system. It has been shown that heliocentric objects impact preferentially on the leading hemisphere of a synchronously rotating satellite, whereas planetocentric impactors weakly favor the apex or antapex [*Dones et al.*, 2009; *Horedt and Neukum*, 1984; *Shoemaker and Wolfe*, 1982]. Previous theoretical studies [*Horedt and Neukum*, 1984; *Zahnle et al.*, 2001] have estimated that the rate of heliocentric impact cratering at the apex of motion (the center of the leading hemisphere or 90°W at the equator) should be approximately 15–100 times greater than that at the antapex (the center of the trailing hemisphere or 270° W at the equator). The density of impact craters should, therefore, reflect this differential cratering rate unless the satellite has experienced a nonsynchronous rotation or the surfaces have become saturated with impact craters.

The factor of the differential cratering depends on both the satellite's orbital velocity (v_{orb}) and the impactor's encounter velocity with a planet (v_∞). According to *Zahnle et al.* [2001], relative crater production as a function of the angle β from the apex of motion can be expressed as follows:

$$\dot{N} \propto \left(1 + \frac{v_{\mathrm{orb}}}{\sqrt{2v_{\mathrm{orb}}^2 + v_\infty^2}} \cos\beta \right)^{2.8} . \quad (1)$$

Specifically, the asymmetry is largest for impactors in orbit around the same primary object or those moving at a low relative velocity [*Melosh*, 2011; *Zahnle et al.*, 2001]. For example, in the Saturn system, v_{orb} is 10 km/s for Rhea and 3 km/s for Iapetus, and *Zahnle et al.* [2003] assume that the median v_∞ is 5 km/s for ecliptic bodies such as Centaurs or Kuiper belt objects and 20 km/s for isotropic objects such as Oort cloud comets. If, following *Zahnle et al.* [2001], a global measure of apex-antapex cratering asymmetry (GMAACA) is defined

Table 1. GMAACA of Craters on Rhea and Iapetus[a]

	Rhea (v_{orb} = 10 km/s)	Iapetus (v_{orb} = 3 km/s)
	Observed	
$D > 50$ km	2.57 ± 0.51	2.75 ± 0.71
50 km $> D >$ 30 km	5.56 ± 0.72	2.17 ± 0.50
30 km $> D >$ 20 km	2.03 ± 0.20	
20 km $> D >$ 15 km	1.63 ± 0.16	
	Theoretical Estimate	
Ecliptic (v = 5 km/s)	40	10
Isotropic (v = 20 km/s)	7.9	2.0

[a]Error is defined by ±(GMAACA)*($N_{leading} + N_{trailing}$)$^{-0.5}$, where $N_{leading}$ and $N_{trailing}$ represent the number of craters within 30° of the apex and antapex, respectively.

by counting only those craters that fall within 30° of the apex or antapex, then the predicted GMAACA for Rhea is 40 for ecliptic comets and 7.9 for isotropic comets, and that for Iapetus is 10 for ecliptic comets and 2.0 for isotropic comets (Table 1).

Despite this prediction, strong asymmetries have not been identified on any of the satellites in the outer solar system. For example, *Smith et al.* [1981] and *Lissauer et al.* [1988] reported that Mimas and Rhea show no apex-antapex asymmetry, based on the Voyager data. In the Jovian system, Ganymede exhibits a fourfold difference between crater densities at its apex and antapex, while Callisto shows no significant asymmetry [*Zahnle et al.*, 2001]. *Leliwa-Kopystynski et al.* [2012] examined the densities of small craters, with diameters of less than 15 km, on Saturnian satellites, and reported no obvious asymmetry on any of the satellite bodies. Finally, *Kirchoff and Schenk* [2010] examined the distribution of craters on Mimas, Tethys, Dione, Rhea, and Iapetus, using the data from Cassini; they did not report apex-antapex asymmetry.

2. Methods

Following the approach of previous studies, this investigation measures craters on Rhea and Iapetus (Figure 1). Rhea and Iapetus, the second and third largest satellites in the Saturn system, are suitable targets for this type of

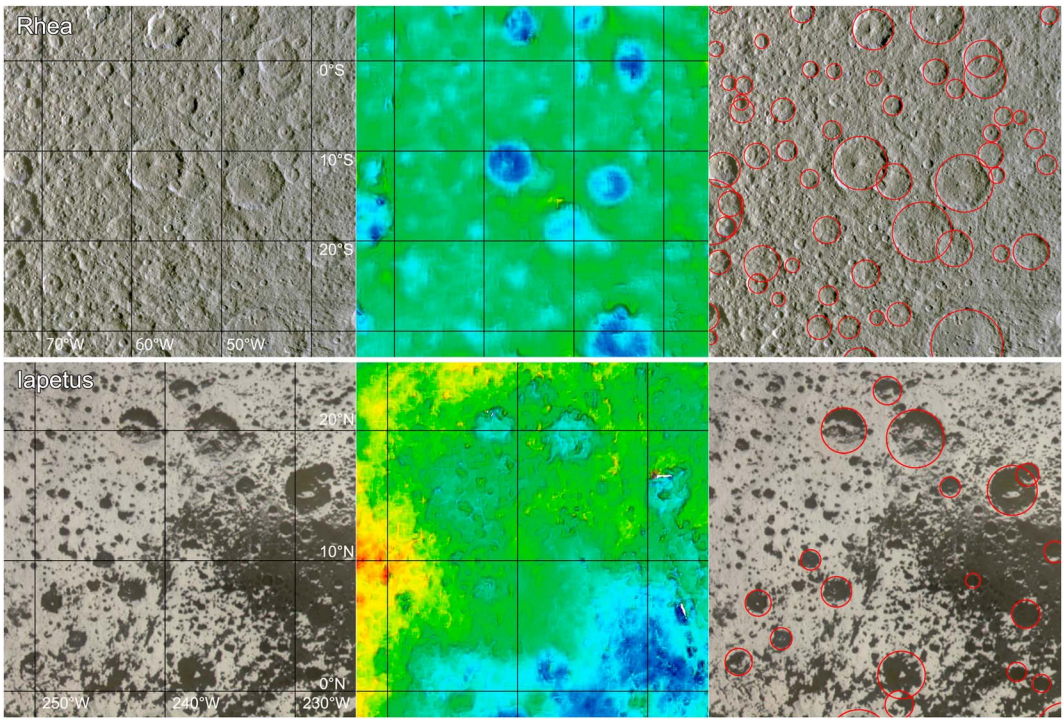

Figure 1. Identification of impact craters of (top row) Rhea and (bottom row) Iapetus. (left column) Global mosaic, (middle column) digital elevation models, and (right column) identified craters.

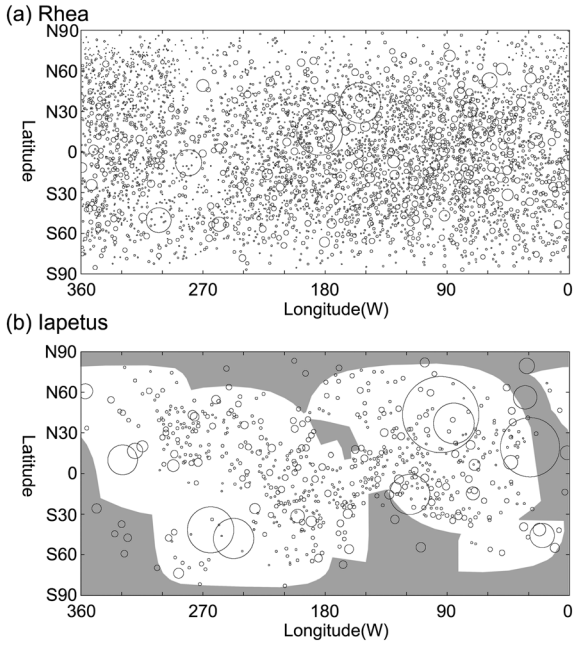

Figure 2. Distributions of craters on the surfaces of (a) Rhea and (b) Iapetus shown in simple cylindrical projection. The size of circles represents the craters' diameter normalized by the scale along its latitude. Grey regions indicate areas with image pixel scales greater than 1 km.

study. Rhea and Iapetus are generally considered to be inert satellites, which is suggested by the undifferentiated interior of Rhea [*Anderson and Schubert*, 2007] and the oblate spheroid shape of Iapetus [*Thomas et al.*, 2007] among other factors. Thus, geologic uniformity of the surfaces is plausibly expected. In contrast, Enceladus, Tethys, Dione, and Titan would be unsuitable because these satellites have experienced endogenic resurfacing processes acting at different times and places. Although Mimas is also considered to be an inert satellite, it is unsuitable target owing to its small surface area and consequently small number of large craters.

2.1. Data

This study combines the data from several sources. First, recently acquired global satellite maps available from NASA's Photojournal, specifically images PIA18438 for Rhea and PIA18436 for Iapetus, are used. Both maps are developed by Dr. Paul Schenk and released in 2014. Pixel scale for both maps is 400 m per pixel, though resolutions of original raw images on Rhea vary from 1.5 to 0.16 km, and on Iapetus, they vary from 7.9 to 0.2 km.

Some parts of these maps are unsuitable for the identification of craters mainly because the composite images were captured with a high angle of solar illumination. Therefore, to analyze these regions of Rhea, seven individual images (shown in Figure S1 and Table S3 in the supporting information) obtained by the imaging science system (ISS) camera on board the Cassini spacecraft are used instead. Unfortunately, some parts of Iapetus have only been imaged at high solar illumination angles, and therefore, no useful individual ISS images were available for Iapetus. The images are freely available from NASA's Planetary Data System. To calibrate these images, the ISIS 3 software produced by the U.S. Geological Survey (USGS) was used. In detail, the application *spiceinit* was used to compute ground positions (latitude and longitude) and *cam2map* was used to project an image to a simple cylindrical projection. The locations of craters on the individual images processed through ISIS 3 are often slightly different from the Photojournal maps. This study aligned the individual images with the Photojournal maps to assure that crater locations are consistent.

Additionally, the regional digital elevation models (DEMs) of Rhea and Iapetus, which can be derived from the NASA Ames Stereo Pipeline software [*Broxton and Edwards*, 2008; *Moratto et al.*, 2010], are produced in this study to support identifications of impact craters (Figures S2 and S3 in the supporting information). These regional DEMs, developed from 25 stereo pairs for Rhea and 26 stereo pairs for Iapetus (Tables S3 and S4), cover 93% of the surface of Rhea and 52% of the surface of Iapetus. Details of the regional DEMs are described in the supporting information.

2.2. Measurements of Impact Craters

The craters are generally measured from the global maps available in NASA's Photojournal. The Cassini ISS camera has almost imaged the entire surface of Rhea at a resolution of 1 km/pixel or higher, in addition to 79% of the surface of Iapetus at the same resolution. In order to measure the diameters and locations of the impact craters, this investigation utilizes the Java Mission-planning and Analysis for Remote Sensing (JMARS) program. It should be noted that JMARS cannot be used to quantify the noncircular craters, and therefore, the mean of the major and minor axes is approximately taken as the diameter of an elliptical crater.

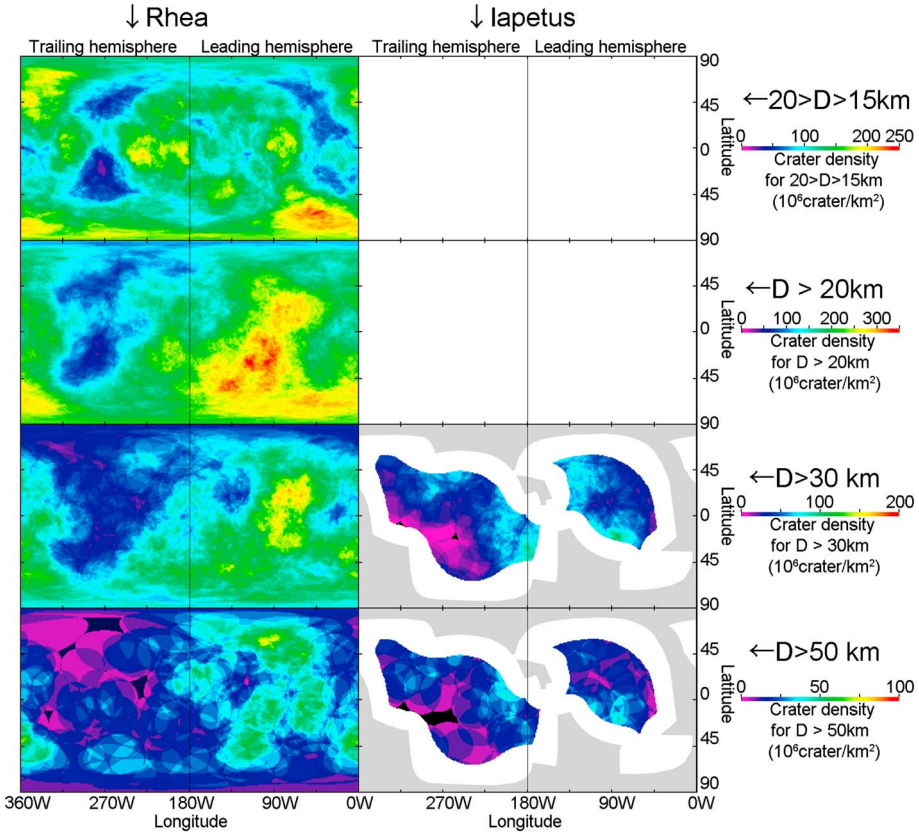

Figure 3. Spatial distribution of the density of craters between 15 km and 20 km and exceeding 20 km, 30 km, and 50 km in diameter (from top to bottom) for (left) Rhea and (right) Iapetus. The density is defined by the area and the number of craters within the circle of colatitude = 20°. Warmer colors indicated by the scale bars mean higher densities.

The criteria for the identification of an impact crater include the following: (i) a circular or elliptical depression with a rim and/or a central peak (central peaks are typically seen in the impact craters larger than around 20 km in diameter on Saturnian midsized satellites) and (ii) features being resolved by at least 15 pixels to enable the most accurate measurements. The resolutions of the images used, therefore, allow the detection of almost all craters more than 15 km in diameter across Rhea. Identifications of depressions, rims, and peaks are verified with DEMs. As mentioned above, images of Iapetus are inferior in quality, and therefore, the identification accuracy of craters less than 30 km in diameter is not uniform across the entire satellite. As a result, 4220 craters are identified for Rhea and Iapetus (Figure 2 and supporting information Table S1 for Rhea and Table S2 for Iapetus).

3. Results

3.1. Rhea

A total of 1373 craters greater than 20 km in diameter were identified on the surface of Rhea (Figure 2a), and their distribution appears to show an apex-antapex asymmetry. The density of large craters ($D > 30$ km) around the apex is approximately 150 (maximum 167) craters/10^6 km^2, while around the antapex it is roughly 30 (minimum 14) craters/10^6 km^2 (Figure 3), where density is defined by the area and craters within the circle of colatitude of 20°. Thus, there is almost a tenfold difference (minimum fivefold and maximum twelvefold) between the apex and antapex regions. The GMAACAs, depending on the size of craters, range between 2.0 and 5.5, as shown in Table 1, which indicates that all larger craters on Rhea (>20 km, 30 km, and 50 km) show the same tendency. Apart from craters smaller than 20 km in diameter, crater density, as a function of the angle measured from the apex of motion, decreases as the angle increases (Figure 4a). In contrast, 871 small craters were identified (15 km $< D <$ 20 km), which do not show the same asymmetry (Figure 3). The GMAACA of Rhea for 15 km $< D <$ 20 km is 1.6.

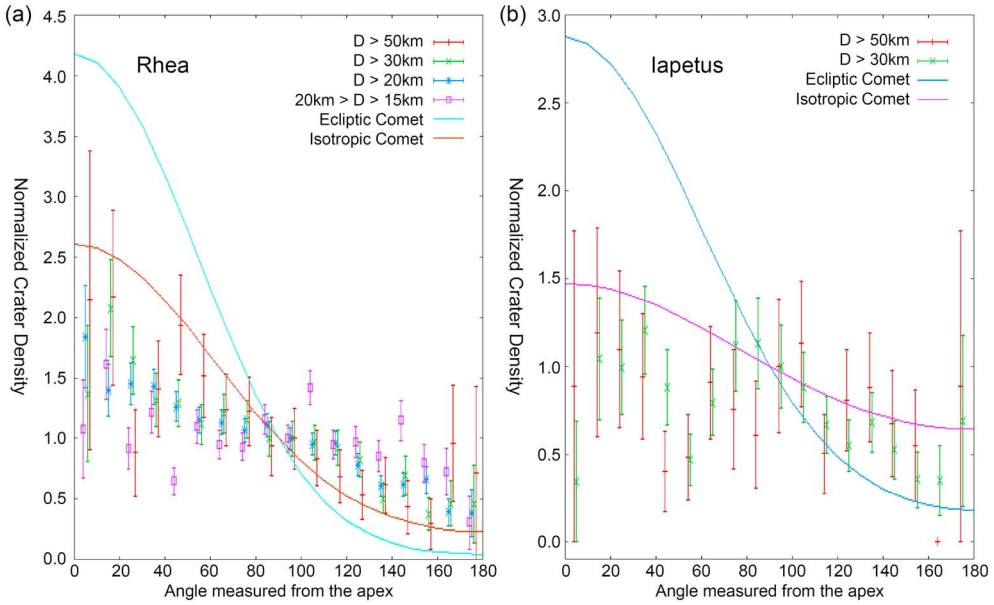

Figure 4. Normalized crater densities of (a) Rhea and (b) Iapetus as functions of the angle measured from the apex of motion. The vertical axis is the relative crater densities normalized to the value at 90°. The error bars are defined as $\pm D^{*}N^{-0.5}$, where D and N are the density and the number of craters in a bin. For crater densities of Iapetus, the grey regions shown in Figure 2 are excluded.

3.2. Iapetus

In total, 259 craters ($D > 30$ km) are reliably identified on 79% of the surface of Iapetus (Figure 2b). The density of large craters ($D > 30$ km) around the apex is approximately 60 craters/10^6 km^2, while around the antapex, it is roughly 20 craters/10^6 km^2 (Figure 3), where the density is defined by the area and craters within the circle of colatitude of 20°. This distribution of craters implies an approximately threefold difference between the apex and antapex regions. GMAACAs depending on the size of the craters for Iapetus are 2.1–2.7 (Table 1), and therefore, the distribution appears to show some degree of apex-antapex asymmetry. However, the crater density on Iapetus, as a function of the angle measured from the apex of motion, is dissimilar to the theoretical estimates (Figure 4b).

4. Discussion

4.1. Craters Larger Than 20 km in Diameter

The apex-antapex asymmetry is observed for the large craters ($D > 20$ km) of Rhea. Even though local resurfacing owing to past endogenic activity on Rhea cannot be ruled out, it is suggested that these large craters are likely dominantly derived from the impacts of heliocentric objects. The crater density, as a function of the angle measured from the apex, is consistent with a heliocentric origin of the impactors; this is expected to be a cosine function (Figure 4a). Moreover, in principle, large craters exceeding 20 km in diameter in the Saturn system are expected to have dominantly heliocentric origins [*Alvarellos et al.*, 2005], excluding the intermittent catastrophic disruptions of satellites, as (i) the maximum size of secondary craters is approximately 4% of the primary crater diameters [*Melosh*, 2011] and (ii) the largest impact basins observed do not exceed 500 km diameter [*Moore et al.*, 2004].

Based on the GMAACA of Iapetus, a weak apex-antapex asymmetry is potentially observed for the large craters ($D > 30$ km) of Iapetus. Thus, the large craters on Iapetus also seem to be dominantly derived from the impacts of heliocentric objects, as well as Rhea. On the other hand, apex-antapex asymmetry for Iapetus is weak and the crater density, as a function of the angle measured from the apex, is not consistent with the theoretical estimates. Finally, the observations for Iapetus may be explained by local resurfacing owing to past endogenic activities and large impacts or measurement error owing to inferior quality of data collection from Iapetus.

Additionally, Pearson's chi-square test is used for statistically comparing the observed crater densities of Iapetus and Rhea with the expected theoretical values derived from equation (1). The test can determine how far off the data are from the null hypothesis of no asymmetry. Details of the test are described in the supporting information. The test for Iapetus indicates that at 95% significance level, the case of isotropic comets is more plausible than the case of no asymmetry. The test for Rhea indicates again that the larger craters show an apex-antapex asymmetry, while the smaller craters show no asymmetry.

The observed GMAACA and the crater densities measured from the apex of both Rhea and Iapetus are, if anything, consistent with the case of isotropic comets. However, ecliptic comets may also be plausible dominant impactors because the leading sides of these satellites plausibly reach saturation with impact craters, causing the observed ratio to be much lower than the expected production.

4.2. Craters Smaller Than 20 km in Diameter

Craters 15 km $< D <$ 20 km do not seem to show asymmetry on Rhea. According to *Leliwa-Kopystynski et al.* [2012], the local densities of the crater $D <$ 15 km on Rhea and Iapetus also show no apex-antapex asymmetry. Thus, the craters less than 20 km in diameter seem to show no significant asymmetry. This lack of asymmetry can either be attributed to the saturation with impact craters or the dominance of planetocentric impactors as the source of these small craters.

The simplest explanation for the lack of asymmetry may be the distinct population, such as planetocentric impactors. Planetocentric impactors can play a major role in the production of small craters in both hemispheres. In addition, the largest crater derived from planetocentric debris is around 20 km in diameter [*Alvarellos et al.*, 2005], which would explain the difference between the distribution of craters with $D <$ 20 km and $D >$ 20 km. Otherwise, the saturation due to heavy cratering of impactors may contribute to the lack of asymmetry. For example, numerous impactors reduce the number of small craters and the saturation of numerous small craters can equalize the observed density between both hemispheres. Thus, no asymmetry for small craters would be explained by a single impactor population, as suggested by *Lissauer et al.* [1988].

4.3. Implications for the Geology of Satellites

Large impactors appear to have barely struck the trailing hemisphere of a satellite over its history, while they must have heavily struck the leading hemisphere. As predicted by *Zahnle et al.* [2001], this work indicates that any ages derived from the density of large craters ($D >$ 20 km) must take the angle bearing from the apex point into account. For example, the ages of Dione's smooth plains (on the leading side) and the unnamed large impact basin (on the trailing side) are estimated to be 1.7 Ga and 2.4 Ga [*Kirchoff and Schenk*, 2015]; however, this apex-antapex relationship would imply that the true ages are younger and older. The trailing hemisphere of Tethys, called the smooth cratered plains [*Wagner et al.*, 2013] or plain terrain [*Moore and Ahern*, 1983], has been considered to be a relatively young terrain; however, its little cratered state could instead be explained by the differential cratering rates. Moreover, the current theoretical cratering rate in the Saturn system, assuming an ecliptic comet origin for major impactors, may be unadoptable for the small craters.

4.4. Comparison With Previous Voyager Era Studies

Previous studies, conducted during the Voyager era [*Horedt and Neukum*, 1984; *Shoemaker and Wolfe*, 1981; *Smith et al.*, 1982] suggested the existence of two types of impactor populations, known as Populations 1 and 2, whose sources were considered to be ecliptic comets and planetocentric debris, respectively. Populations 1 and 2 were suggested to be expressed on heavily cratered terrains, which are characterized by an abundance of craters larger than 20 km in diameter, and younger terrains, which are characterized by a deficiency of craters larger than 20 km, respectively [*Smith et al.*, 1982]. Generally, it was thought that Population 1 was responsible for forming large, old craters, while Population 2 formed small, young craters.

This study indicates that Population 1 (large craters) may be consistent with a heliocentric origin due to their observed apex-antapex asymmetry, while Population 2 (small craters) may either be in saturation or is planetocentric in origin due to the absence of an observed apex-antapex asymmetry, in agreement with previous studies [e.g., *Smith et al.*, 1982]. However, the results obtained in this study suggest that there may be no change with time. This study implies that the accumulation of heliocentric impacts on the leading

hemisphere over time may form terrains characterized by Population 1. In addition, the heliocentric large impactors seem to have currently struck the surface of satellites. Relatively young impact basins, such as Odysseus and Evander basins, support this view. Thus, Population 1 can be young. The accumulation of planetocentric impacts on the trailing hemisphere over time may form terrains with numerous small craters and without large craters. Terrains characterized by Population 2 may belong to not only young terrains but also old terrains lying on the trailing hemisphere, such as that of Tethys or Rhea. Thus, Population 2 can be old.

5. Conclusions

A total of 2244 craters ($D > 15$ km) were identified on Rhea, and 259 craters ($D > 30$ km) were identified on Iapetus. The densities of large craters ($D > 20$ km) on Rhea show apex-antapex asymmetries, while those of small craters (15 km $< D < 20$ km) show no asymmetric distributions. The densities of craters ($D > 30$ km) on Iapetus show relatively small apex-antapex asymmetries. Taking no apex-antapex asymmetry for the local densities of small craters ($D < 15$ km) [*Leliwa-Kopystynski et al.*, 2012] into consideration, it is suggested that the larger craters ($D > 20$ km) show an apex-antapex asymmetry, while the smaller craters ($D < 20$ km) seem to show no asymmetry. This difference is likely a result of heliocentric impactors playing a major role in forming large craters, while planetocentric impactors produce a majority of small craters. The surface ages derived by the density of large craters ($D > 20$ km) must consider the angle bearing from the apex point, while the surface ages derived by the density of small craters ($D < 20$ km) may be much different from the estimates based on the heliocentric origins. Finally, results indicate that Populations 1 and 2 proposed in the Voyager era studies correspond to heliocentric and planetocentric impactors. However, this work suggests that there may be no change with time, in contract with the Voyager era studies, which hypothesized that Population 1 was old and Population 2 was young.

Acknowledgments

The author wishes to thank David Minton and Michelle Kirchoff for their comments, which helped to improve this paper significantly. Additionally, this work is supported by Grant-in-Aid for JSPS fellows. Raw image data are freely available via NASA's Planetary Data System (http://pds.nasa.gov), and mosaic images are released as a part of NASA's Photojournal (http://photojournal.jpl.nasa.gov/). Additionally, Ames Stereo Pipeline software and ISIS 3 software are freely available at NASA (http://ti.arc.nasa.gov/tech/asr/intelligent-robotics/ngt/stereo/) and USGS (http://isis.astrogeology.usgs.gov/) websites, respectively. For crater counting, the JMARS software provided by USGS (https://jmars.asu.edu/) was used.

References

Alvarellos, J. L., K. J. Zahnle, A. R. Dobrovolskis, and P. Hamill (2005), Fates of satellite ejecta in the Saturn system, *Icarus*, *178*(1), 104–123, doi:10.1016/j.icarus.2005.04.017.

Anderson, J. D., and G. Schubert (2007), Saturn's satellite Rhea is a homogeneous mix of rock and ice, *Geophys. Res. Lett.*, *34*, L02202, doi:10.1029/2006GL028100.

Bierhaus, E. B., L. Dones, J. L. Alvarellos, and K. Zahnle (2012), The role of ejecta in the small crater populations on the mid-sized Saturnian satellites, *Icarus*, *218*(1), 602–621.

Broxton, M. J., and L. J. Edwards (2008), The Ames Stereo Pipeline: Automated 3D surface reconstruction from orbital imagery, 39th Lunar and Planetary Science Conference, Abstract 2419, Lunar and Planetary Institute, Houston.

Dones, L., C. R. Chapman, W. B. McKinnon, H. J. Melosh, M. R. Kirchoff, G. Neukum, and K. J. Zahnle (2009), Icy satellites of Saturn: Impact cratering and age determination, in *Saturn From Cassini-Huygens*, pp. 613–635, Springer, Netherlands.

Horedt, G., and G. Neukum (1984), Planetocentric versus heliocentric impacts in the Jovian and Saturnian satellite system, *J. Geophys. Res.*, *89*(B12), 10,405–10,410, doi:10.1029/JB089iB12p10405.

Kirchoff, M. R., and P. Schenk (2010), Impact cratering records of the mid-sized, icy Saturnian satellites, *Icarus*, *206*(2), 485–497.

Kirchoff, M. R., and P. Schenk (2015), Dione's resurfacing history as determined from a global impact crater database, *Icarus*, *256*, 78–89.

Leliwa-Kopystynski, J., M. Banaszek, and I. Wlodarczyk (2012), Longitudinal asymmetry of craters' density distributions on the icy satellites, *Planet. Space Sci.*, *60*(1), 181–192.

Lissauer, J. J., S. W. Squyres, and W. K. Hartmann (1988), Bombardment history of the Saturn system, *J. Geophys. Res.*, *93*(B11), 13,776–13,804, doi:10.1029/JB093iB11p13776.

Melosh, H. J. (2011), *Planetary Surface Processes*, Cambridge Univ. Press, Cambridge.

Moore, J. M., and J. L. Ahern (1983), The geology of Tethys, *J. Geophys. Res.*, *88*(S02), A577–A584, doi:10.1029/JB088iS02p0A577.

Moore, J. M., P. M. Schenk, L. S. Bruesch, E. Asphaug, and W. B. McKinnon (2004), Large impact features on middle-sized icy satellites, *Icarus*, *171*(2), 421–443.

Moratto, Z. M., M. J. Broxton, R. A. Beyer, M. Lundy, and K. Husmann (2010), Ames Stereo Pipeline: NASA's open source automated stereogrammetry software, 41st Lunar and Planetary Science Conference, Abstract 2364, Lunar and Planetary Institute, Houston.

Shoemaker, E. M., and R. Wolfe (1981), Evolution of the Saturnian satellites: The role of impact, LPI Contributions, 428, 1.

Shoemaker, E. M., and R. Wolfe (1982), Cratering time scales for the Galilean satellites, in *Satellites of Jupiter*, pp. 277–339, Univ. of Arizona Press, Tucson.

Smith, B. A., L. Soderblom, R. Beebe, J. Boyce, G. Briggs, A. Bunker, S. A. Collins, C. J. Hansen, T. V. Johnson, and J. L. Mitchell (1981), Encounter with Saturn: Voyager 1 imaging science results, *Science*, *212*(4491), 163–191.

Smith, B. A., L. Soderblom, R. Batson, P. Bridges, J. Inge, H. Masursky, E. Shoemaker, R. Beebe, J. Boyce, and G. Briggs (1982), A new look at the Saturn system: The Voyager 2 images, *Science*, *215*(4532), 504–537.

Thomas, P. C., et al. (2007), Shapes of the Saturnian icy satellites and their significance, *Icarus*, *190*(2), 573–584, doi:10.1016/j.icarus.2007.03.012.

Wagner, R. J., K. Stephan, N. Schmedemann, T. Roatsch, E. Kersten, G. Neukum, and C. Porco (2013), Geology and stratigraphy of Saturn's moon Tethys, European Planetary Science Congress 2013, Abstract 713, Univ. College London, London.

Zahnle, K., P. Schenk, S. Sobieszczyk, L. Dones, and H. F. Levison (2001), Differential cratering of synchronously rotating satellites by ecliptic comets, *Icarus*, *153*(1), 111–129.

Zahnle, K., P. Schenk, H. Levison, and L. Dones (2003), Cratering rates in the outer solar system, *Icarus*, *163*(2), 263–289.